European Journal of Operational Research 284 (2020) 345–354

Contents lists available at ScienceDirect

European Journal of Operational Research

journal homepage: www.elsevier.com/locate/ejor

Innovative Applications of O.R.

Optimal control of water distribution networks without storage

Dimitrios Nerantzis*, Filippo Pecci, Ivan Stoianov

InfraSense Labs, Department of Civil and Environmental Engineering, Imperial College London, London SW7 2BB, UK

ARTICLE INFO

Article history:
Received 17 June 2019
Accepted 7 December 2019
Available online 11 December 2019

Keywords:
Networks
Mathematical optimization
Optimal control
Variable speed pumps
Water distribution systems

ABSTRACT

The paper investigates the problem of optimal control of water distribution networks without storage capacity. Using mathematical optimization, we formulate and solve the problem as a non-convex NLP, in order to obtain optimal control curves for both variable speed pumps and pressure reducing valves of the network and thus propose a methodology for the automated control of real operational networks. We consider both single-objective and multi-objective problems with average zonal pressure, pump energy consumption and water treatment cost as objectives. Furthermore, we investigate global optimality bounds for the calculated solutions using global optimization techniques. The proposed approach is shown to outperform state-of-the-art global optimization solvers. The described procedure is demonstrated in a case study using a large size operational network.

1. Introduction

Drinking water distribution systems, especially in large metropolitan areas of the world, are now faced with numerous challenges: Increasing size and complexity, aging infrastructure, increase of urban population, diminishing potable water resources and energy costs. These challenges present the need for advanced control (and design) of water distribution networks, which enable dynamic adaptability both in terms of hydraulic conditions and network connectivity (Wright, Abraham, Parpas, & Stoianov, 2015).

Control of network elements such as valves and pumps, for optimal pressure, leakage and pipe damage reduction and energy cost minimization has been the focus of numerous works in the literature (for example Fooladivanda and Taylor (2018); Ghaddar, Claeys, Mevissen, and Eck (2017); Ghaddar, Naoum-Sawaya, Kishimoto, Taheri, and Eck (2015); León-Celi, Iglesias-Rey, Martínez-Solano, and Savic (2018); Skworcow, Paluszczyszyn, and Ulanicki (2014); Wright et al. (2015)). Furthermore, the use of variable speed pumps (instead of fixed speed) offers greater control and adaptability within a water distribution network, which can increase energy savings and reduce maintenance costs (Page, Abu-Mahfouz, & Mothetha, 2017).

While the presence of tanks provides a number of benefits for the management of WDNs, storage capacity is not always available or the best choice - see Walski and Creaco (2016). Furthermore, it might be the case that, in practice, we consider separately part or parts of a larger network which do not contain any storage capacity.

Wright et al. (2015) use sequential convex programming for the optimal control of pressure reducing valves in order to minimize the average zonal pressure in an operational water network without storage. Based on the optimized solutions, they derived and implemented the optimal control for the valves however, no pump control was considered.

Ghaddar et al. (2017) consider the global optimization of valve settings for the minimization of pressure and apply semidefinite programming relaxations with a branch-and-bound scheme. However, they consider the solution for only one time step (i.e. for a single demand vector).

León-Celi et al. (2018) consider the operation of multiple variable speed pumps in water distribution networks without storage. Using derivative-free optimization methods, they solve the problem of optimal control of the pumps with the sum of power consumption and water treatment cost as the objective function. However, in this case, no valve control was considered and also constant efficiency was assumed for the operation of pumps. Furthermore, the developed pressure management scheme was based on a critical node (i.e. node with the lowest pressure in the network).

The novelties of this work are as follows: Firstly, we consider the simultaneous optimal control of pressure reducing valves and variable speed pumps. Secondly, in contrast with León-Celi et al. (2018), we show that using a simplified modelling of the variable speed pumps, does not mean that the characteristics of the pumps need to be neglected but can be incorporated into the optimization formulation as linear constraints. These constraints correspond

* Corresponding author.
E-mail addresses: dimitrios.nerantzis10@imperial.ac.uk (D. Nerantzis), f.pecci14@imperial.ac.uk (F. Pecci), ivan.stoianov@imperial.ac.uk (I. Stoianov).

https://doi.org/10.1016/j.ejor.2019.12.011
0377-2217/

to a convex polytope approximating the bounds of the required efficiency area of the pumps. Thirdly, we consider how the optimization results can be used in practise for the automatic control of a real, operational network where flow modulation control curves are derived from the optimization results. Finally, we investigate global optimality bounds for the computed solutions. The proposed optimization based bound tightening scheme is shown to outperform both the performance reported in Ghaddar et al. (2017) as well as state-of-the-art solvers such as BARON (Tawarmalani & Sahinidis (2005)).

The structure of the paper is as follows: In Section 2, we introduce the Bristol Water Field Lab (BWFL) network, which we use as our case study. In Section 3, we present the mathematical modelling of WDNs. Modelling the characteristics of variable speed pumps (VSPs) is explained in Section 4. In Section 5, we present the optimization formulation for both single and multi-objective optimal control of the WDN. In Section 6, we discuss our results from the application of the presented optimization formulation to the BWFL network. Finally, we draw our conclusions in Section 7.

2. The BWFL case study network

The Bristol Water Field Lab (BWFL) network is part of the water distribution network of the city of Bristol, UK, and it serves approximately 8,000 customer connections. The BWFL is a unique smart water network demonstrator, where advanced sensing and control solutions have been developed and implemented to enable the dynamically adaptive control for both the hydraulic conditions and network connectivity. It is operated jointly by Bristol Water plc, InfraSense Labs in the Department of Civil and Environmental Engineering at Imperial College London, and Cla-Val Ltd. The BWFL has been used as a case study in a number of publications (for example see Abraham and Stoianov (2017); Pecci, Abraham, and Stoianov (2019); Wright et al. (2015); Wright, Stoianov, Parpas, Henderson, and King (2014)).

The modified hydraulic model of the BWFL network consists of 2013 nodes and 2369 links. Potable water is provided to the network by two inlets (sources), indicated by the square markers in Figure 1. In addition, there are two pressure reducing valves (PRVs), shown by the circle markers and two boundary control valves (BVs), shown by the triangle markers. The boundary control valves open and close according to a pre-determined time schedule (typically between 02:00 and 04:00 hours), which is embedded within the constraints of the optimization problem. The control profiles for the PRVs are derived from the solution of the optimization problem. For the purpose of this investigation, we also modified the BWFL network in order to include two variable speed pumps (VSPs) placed at the two inlets (sources).

3. Water distribution networks – Mathematical modelling

A water distribution network (WDN) is represented as a graph $G(V, E)$. The set of vertices, V, represents the nodes of the network with $|V| = n_n + n_0$ being the total number of nodes. The network model includes n_n unknown head nodes and n_0 source nodes. The set of edges, E, represents the set of links connecting the nodes with $|E| = n_p$ being the number of links. We consider the 24-hour operation of a WDN in n_t discrete time steps.

At each time step, we have a vector of nodal head values, $h \in \mathbb{R}^{n_n}$ (m) and a vector of nodal demands $d \in \mathbb{R}^{n_n}$ (m^3/s). Note that the demand for some nodes can be fixed to zero. For the set of links we have a corresponding vector of flow values $q \in \mathbb{R}^{n_p}$ (m^3/s). We also consider a vector of fixed head values for source nodes, denoted by $h_0 \in \mathbb{R}^{n_0}$. Furthermore, we define the link-node incidence matrix of the WDN, $A_{12} \in \mathbb{R}^{n_p \times n_n}$, as follows:

$$A_{12}(i,j) = \begin{cases} 1 & \text{if link i enters node j} \\ 0 & \text{if link i is not connected to node j.} \\ -1 & \text{if link i leaves node j.} \end{cases} \quad (1)$$

In a similar manner with A_{12}, we define the link-source node incidence matrix, $A_{10} \in \mathbb{R}^{n_p \times n_0}$. In addition, we consider the vector of control variables $u \in \mathbb{R}^{n_u}$ (m) where n_u is the number of PRVs and VSPs. When u_i corresponds to a PRV, it represents the amount of head reduced by the PRV and when it corresponds to a VSP, it represents the head boost provided by the VSP. Finally, we define the matrix $A_{13} \in \mathbb{R}^{n_p \times n_u}$ as follows:

$$A_{13}(i,j) = \begin{cases} 1 & \text{if link i is the PRV corresponding to variable } u_j. \\ 0 & \text{if link i is a pipe.} \\ -1 & \text{if link i is the VSP corresponding to variable } u_j. \end{cases} \quad (2)$$

We consider a demand-driven, steady-state hydraulic model of the network. Thus, we assume that, at each time step, an approximation of the demand vector d is known and we require the mass and energy balance constraints to be satisfied,

$$A_{12}^T q - d = 0 \quad (3)$$

$$A_{12}h + A_{10}h_0 + A_{13}u + A_{11}(q)q = 0, \quad (4)$$

where

$$A_{11}(q) = \text{diag}(a_1|q_1| + b_1, \ldots, a_{n_p}|q_{n_p}| + b_{n_p}). \quad (5)$$

The mass balance given by (3) states that the flow that enters a node must equal the flow that leaves the node. Note that the flows can take negative or positive values with respect to the assumed direction of the corresponding link. The energy balance given by (4), accounts for the energy losses (i.e. head losses) across a link due to the frictional losses which depend on the flow and physical properties of the pipe. The values for a_i and b_i in Eq. (5) are calculated following the work of Bradley J. Eck (2015) and Pecci, Abraham, and Stoianov (2017) in order to approximate the Hazen-Williams head-loss formula for each link.

4. Variable speed pumps (VSPs)

In our experiments we make use of a theoretical pump whose characteristics are based on affinity laws (Walski, Zimmerman, Dudinyak, & Dileepkumar (2003)). Nevertheless, this does not restrict the applicability of the procedure since for a commercial pump we can make use of the data provided by the manufacturer.

The affinity laws describe the proportional relationship of flows, heads and power of a variable speed pump operating between two different speeds, ω_1 and ω_2. They are given by Eq. (6)–(8),

$$\frac{q_1}{q_2} = \frac{\omega_1}{\omega_2} \quad (6)$$

$$\frac{u_1}{u_2} = \left(\frac{\omega_1}{\omega_2}\right)^2 \quad (7)$$

$$\frac{p_1}{p_2} = \left(\frac{\omega_1}{\omega_2}\right)^3 \quad (8)$$

where q_1, u_1, p_1 and q_2, u_2, p_2 are the flows, heads and power consumption of the VSP, corresponding to speeds ω_1 and ω_2 respectively. By choosing the values of flow and head, q^* and u^*, at which the pump operates at maximum efficiency at nominal speed, we define a nominal speed pump curve (i.e. the speed as a proportion

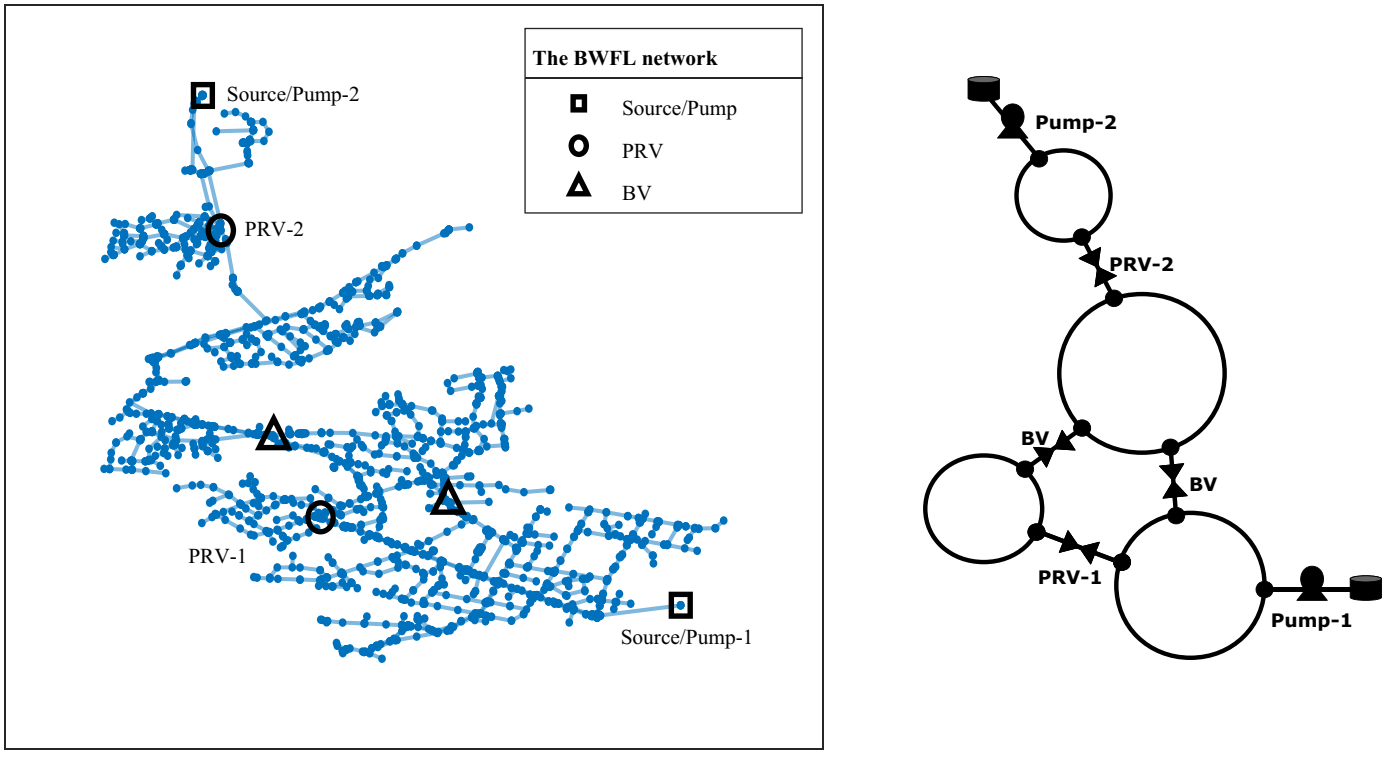

Fig. 1. The Bristol Water Field Lab (BWFL) network (modified for the purposes of our case study).

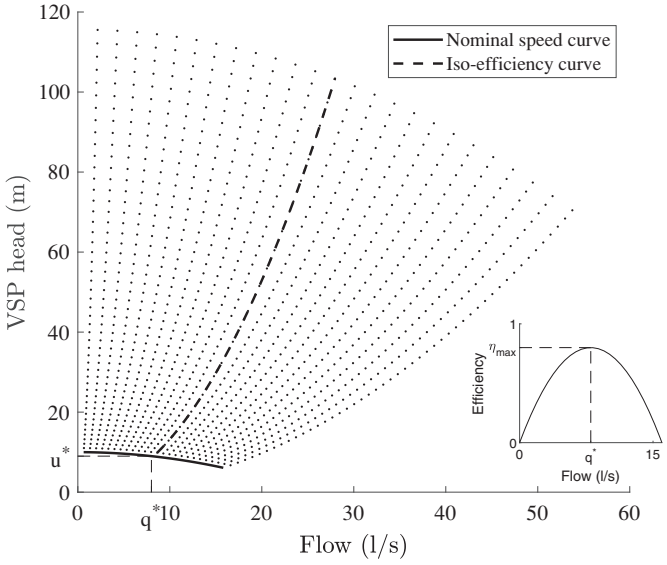

Fig. 2. Variable speed pump curves. The efficiency curve, corresponding to the nominal speed, is shown in the smaller graph.

of which we consider any other operating speed of the pump) of the form,

$$u(q) = aq^2 + b \tag{9}$$

where $a = (u^* - b)/q^{*2}$ (such that $u(q^*) = u^*$) and b determines the intersection of the nominal speed curve with the head axis. Next, we define a corresponding efficiency curve of the form,

$$\eta(q) = -c(q - q^*)^2 + \eta_{max}, \tag{10}$$

where η_{max} is the maximum efficiency of the pump. For our experiments we have used $q^* = 8$ (l/s), $u^* = 9$ (m), $b = 10$ and $\eta_{max} = 0.8$ for both VSPs. The value of c in Eq. (10) is chosen such that $\eta(0) = 0$ and thus $c = \eta_{max}/q^{*2}$.

With the nominal speed and efficiency curves defined in Eqs. (11) and (12) respectively and by employing the affinity laws, we can determine the pump curves for any throttle speed with respect to the throttle speed of the nominal curve. This is shown in Figure 2.

Moreover, we can calculate the efficiency and the power consumption for given pump flow and head values. This will allow us to include efficiency constraints in our optimization formulation (Section 5) as well as to consider energy consumption as an objective function (Section 6).

Finally, it is important to note that the speed of a VSP can vary continuously within a certain range (Brdys & Ulanicki (1994)). The points depicted in Figure 2 show only the corresponding curves for a discrete set of operating speeds. Therefore, for any flow-head pair (q, u) there is a speed for which the corresponding pump curve passes through (q, u) (as long as the pair (q, u) is within the operational limits of the pump).

5. Mathematical optimization – Problem formulation

5.1. Objective functions

We consider the 24-hour optimal control of the network with respect to average zonal pressure (AZP), energy consumption (EC) and water treatment cost (WTC). The corresponding formulation for each objective is given in Eqs. (11)–(13) where, $x = [x_1, ..., x_{n_t}]^T$ with $x_t = [q_t \ h_t \ u_t]^T$ for $t = 1, ..., n_t$.

Average Zonal Pressure (AZP):

One of the most important aspects of control in a WDN is nodal pressure. By operating a network with as low pressure as possible we can reduce leakage, pipe damage and burst incident rates (Lambert & Thornton (2011)). Hence, we will consider pressure as our first objective for optimal control of the WDN. A standard metric of pressure in a network is the Average Zonal Pressure

(AZP):

$$f_{AZP}(x) = \frac{1}{n_t}\sum_{t=1}^{n_t}\sum_{j=1}^{n_n}\alpha_j(h_j^{(t)} - \xi_j) \tag{11}$$

where $\alpha_j = \sum_{j\in I_j} L_j/(2\bar{L})$ with I_j being the set of pipe indices of pipes connected to node j, L_j the length of pipe j, $\bar{L}$ the average pipe length in the network and ξ_j the elevation of node j. The AZP is thus a weighted average of pressure in the network where the weighting is with respect to the length of pipes connected to each node.

Energy Consumption (EC):

$$f_{EC}(x) = \sum_{t=1}^{n_t}\sum_{j\in I_{\text{pumps}}}^{n_{\text{pumps}}}\frac{\gamma\ q_j^{(t)}\,u_j^{(t)}}{\eta\left(q_j^{(t)}, u_j^{(t)}\right)}\delta t\ \ (kWh) \tag{12}$$

where n_{pumps} is the number of pumps in the network, I_{pumps} is the set of pump link indices, q_j is the flow through link j, u_j is the discharge head of the corresponding pump, $\gamma = 9.81$ (kiloNewton/meter^3) is the specific weight of water, and δt is the time-step duration in hours (in our case $\delta t = 1/4$ (h)). In addition, $\eta(q_j, u_j)$ is the efficiency of the pump when operating at (q_j, u_j).

Given q_j and u_j, using the affinity laws and Eq. (9), of the nominal curve, we can calculate the flow for which, at nominal speed, the pump has the same efficiency as when operating at q_j and u_j and thus, using the efficiency curve (10) calculate $\eta(q_j, u_j)$ and finally the energy consumption at q_j and u_j.

For our experiments, we have fitted a quadratic polynomial in order to obtain an approximation of the surface of the energy consumption and use it as our objective function. This, resulted in a convex quadratic polynomial and thus more convenient, with respect to optimization, compared to a more complicated closed formula for the energy consumption.

Water Treatment Cost (WTC):

$$f_{WTC}(x) = \sum_{t=1}^{n_t}\sum_{i\in I_{source}}^{n_0} q_i^{(t)}c_i^{(t)}\ \delta t \tag{13}$$

where, n_t is the number of time-steps, n_0 is the number of sources/reservoirs in the network, $q_i^{(t)}$ is the outgoing flow from source i at time-step t, $c_i^{(t)}$ (£/m^3) is the water treatment cost per m^3 from source i at time-step t and δt (s) is the duration of each time-step in seconds. For our experiments we have used $c_1^{(t)} = 0.15$ (£/m^3) and $c_2^{(t)} = 0.35$ (£/m^3) for all $t = 1, 2, ..., n_t$.

5.2. Single-objective optimization

The general form of the single-objective optimization problem that we aim to solve is given in Problem 1:

Problem 1 (P1):

$$\begin{aligned}
\min\quad & f(x)\\
\text{s.t.}\quad & A_{12}^T q_t - d_t = 0 && \text{(Mass balance)}\\
& A_{12}h_t + A_{10}h_0 + A_{13}u_t + A_{11}(q_t)q_t = 0 && \text{(Energy balance)}\\
& q_{min} \le q_t \le q_{max},\ \ h_{min} \le h_t \le h_{max}\\
& u_t \ge 0\\
& t = 1, ..., n_t.
\end{aligned}$$

where $x = [x_1 ... x_{n_t}]^T \in \mathbb{R}^{(n_p+n_n+n_u)n_t}$. Note that, due to the form of the terms $A_{11}(q_t)q_t$, P1 is a non-linear, non-convex program.

Because the constraints in P1 are decoupled with respect to time and the objective functions presented in Section 5.1 are separable with respect to time, problem P1 can be solved separately for each time-step (and thus in parallel if needed). Furthermore, we note that if storage elements, i.e. tanks, where present in the network this would no longer be true since the tank constraints would be coupled in time.

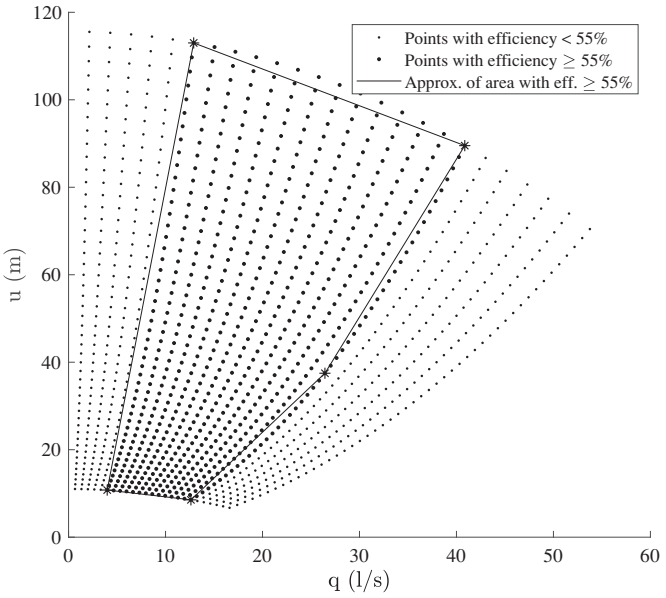

Fig. 3. Approximation of the required efficiency area by a convex polytope.

The formulation of P1 does not take into account any characteristics of the pumps. Specifically, efficiency bounds within which the pumps are allowed to operate (i.e. bounds for the u_i control variables which correspond to pumps). These bounds can be due to the actual operational limits of the pumps or in order to prevent wear down and damage. Another reason for such bounds can be to reduce energy consumption however, improving efficiency does not necessarily lead to lower energy consumption.

Given a minimum efficiency threshold, we can impose efficiency bounds, as linear constraints, $Kq_t + \Lambda u_t \le b$, in our problem formulation, approximating the allowed area of operation by a convex polytope with n_{poly} edges (and n_{vsp} being the number of VSPs in the network). Where, $K \in \mathbb{R}^{n_{poly}n_{vsp}\times n_p}$, $\Lambda \in \mathbb{R}^{n_{poly}n_{vsp}\times n_u}$, $b \in \mathbb{R}^{n_{poly}n_{vsp}}$. This is shown in Fig. 3 and the new formulation is given in Problem 2.

Problem 2 (P2):

$$\begin{aligned}
\min\quad & f(x)\\
\text{s.t.}\quad & A_{12}^T q_t - d_t = 0 && \text{(Mass balance)}\\
& A_{12}h_t + A_{10}h_0 + A_{13}u_t + A_{11}(q_t)q_t = 0 && \text{(Energy balance)}\\
& Kq_t + \Lambda u_t \le b && \text{(Efficiency constraints)}\\
& q_{min} \le q_t \le q_{max},\ \ h_{min} \le h_t \le h_{max}\\
& u_t \ge 0\\
& t = 1, ..., n_t.
\end{aligned}$$

The entries of K, Λ and b are calculated after choosing appropriate points on the plane (q, u) that define the approximating convex polytope for each pump. The number and location of points can vary based on our choice. In our case, the chosen points and the corresponding convex polytope (the same for both pumps) are shown in Figure 3.

It is possible that, for given efficiency bounds, P2 might be infeasible. One option would be to relax/enlarge the convex polytope. However, this might result in a number of previously feasible points $(q_j^{(t)}, u_j^{(t)})$ to move to an area of lower efficiency. Therefore, a better approach would be to include a slack vector, $s_t \ge 0$, allowing for violation of the efficiency constraints, $Kq_t + \Lambda u_t - s_t \le b$, while adding a penalty function $g(s_1, ..., s_{n_t})$ to the objective.

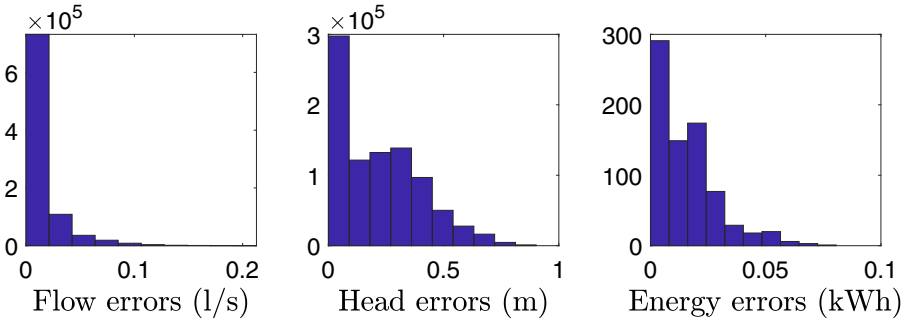

Fig. 4. Absolute errors/differences for flows, heads and energy consumption between hydraulic simulation and optimization results for the BWFL network.

Nevertheless, in our results from the study case presented in Section 6, we make use of formulation P2 since it is simpler and feasible for the considered network.

It is important to note that the modelling of VSPs in the formulation of P2 is advantageous compared to other approaches used in the literature (for example D'Ambrosio, Lodi, Wiese, and Bragalli (2015); Fooladivanda and Taylor (2018)) where formulas of the VSP curves are included directly in the energy balance constrain and include a variable for the pump speed. The modelling of each VSP in P2, by a linear control variable, offers a benefit with respect to optimization while at the same time and in contrast with León-Celi et al. (2018) the characteristics of the pumps are not being neglected.

5.3. Multi-objective optimization

We also consider a multi-objective optimal control of the WDN. In Section 6, we present the results from the optimal control of the BWFL network with average zonal pressure and water treatment cost as the objectives.

The most widely known methods for calculating the Pareto front of a multi-objective problem are the Weighted Sum (Miettinen, 1998), the Normal Boundary Intersection (Das & Dennis, 1998) and the Normalized Normal Constraint method (Messac, Ismail-Yahaya, & Mattson, 2003). All the aforementioned methods solve a series of single-objective problems in order to calculate points of the Pareto front.

In our case, we implement the Normalized Boundary Intersection (NBI) method. Thus, for a given vector $w = [w_1, w_2]^T$, where $w_1, w_2 \geq 0$ and $w_1 + w_2 = 1$ we require the solution of Problem 3:

Problem 3 (P3):

$$
\begin{aligned}
\min \quad & -s \\
\text{s.t.} \quad & f^*_{AZP} + L_{12} w_2 + s Q_1 = f_{AZP}(x) \\
& f^*_{WTC} + L_{21} w_1 + s Q_2 = f_{WTC}(x) \\
& A_{12}^T q_t - d_t = 0 \qquad \text{(Mass balance)} \\
& A_{12} h_t + A_{10} h_0 + A_{13} u_t + A_{11}(q_t) q_t = 0 \quad \text{(Energy balance)} \\
& q_{min} \leq q_t \leq q_{max}, \;\; h_{min} \leq h_t \leq h_{max} \\
& u_t \geq 0, \;\; s \geq 0 \\
& t = 1, 2, \ldots, n_t, \;\; x \in \mathbb{R}^{(n_p + n_n + n_u) n_t}
\end{aligned}
$$

where f^*_{AZP}, f^*_{WTC} are the (global) minima of the corresponding single-objective problems and by denoting with x^*_{AZP}, x^*_{WTC} the corresponding minimizers we define the entries of matrix L as $L_{11} = L_{22} = 0$, $L_{12} = f_{AZP}(x^*_{WTC}) - f^*_{AZP}$ and $L_{21} = f_{WTC}(x^*_{AZP}) - f^*_{WTC}$. Finally, we define as $Q = -L\mathbf{1}_n$ the quasi-normal vector pointing towards the "utopia point" $[f^*_{AZP}\ f^*_{WTC}]^T$. In addition, we can include the VSP efficiency constrains in the formulations of P3. Note that, in contrast with P1 and P2, in the formulation of P3 the first two constraints couple the problem in time (since f_{AZP} and f_{WTC} involve all time-steps"). Thus, P3 must be solved considering all time-steps.

6. Results

In this section we present the results from the implementation of the modelling (Sections 3,4) and optimization formulations (Section 5) on the Bristol Water Field Lab (BWFL) network introduced in Section 2. Further implementation of the presented methodologies to another network can be found in the Supplementary Material.

All numerical experiments were conducted on a Windows 10 Enterprise (64-bit), Intel(R) Xeon(R) CPU E5-2665 @2.40 GHz, 32GB RAM system. For the (local) solutions of the optimization problems we have used IPOPT (Wächter & Biegler, 2006) with Matlab R2018a. The solution of the single objective problems, P1 and P2, for a single time-step, took approximately 1 second. Calculation of a single Pareto front point (solving Problem P3) took on average 6 minutes. As a linear solver we use CPLEX v12.8 (www.cplex.com). Finally, we make use of two global solvers, BARON v19.3.24 (Tawarmalani & Sahinidis (2005)) and SCIP v5.0.1 (Gleixner et al. (2017)).

The results shown in Figs. 5,6 and 8,9 are results from hydraulic simulations (the hydraulic simulation method was based on Abraham and Stoianov (2015, 2017) where a detailed comparison with the EPANET hydraulic simulator can also be found) using the control variable settings obtained from the optimization results. The hydraulic simulation allows us to obtain more accurate results since in the optimization formulation we use an approximation of the Hazen-Williams formula while the hydraulic simulation uses the exact formula. The absolute errors/differences in the results between simulation and optimization are shown in Fig. 4.

6.1. Single-objective optimal control

In Fig. 5, we show the results from the optimal 24-hour operation of the WDN, acquired by solving problems P1 (no efficiency constraints) and P2 (efficiency constraints) with AZP as the objective function. The minimum pressure head as defined by the regulatory compliance threshold is 15 m. The first row of sub-figures corresponds to the solution of P1 and the second to the solution of P2.

By comparing the two rows of sub-figures, we observe that, as expected, when the network is operated with the efficiency constraints, the AZP takes slightly higher values (maximum increase $\approx$1.5 m). Nevertheless, this small increase in the AZP is acceptable with respect to the operation of the network. On the other hand, the total power consumption is slightly lower (6 *kWh* less, over the 24-hour operation). Furthermore, we observe that there is higher variation in the outlet head of the PRVs when the efficiency

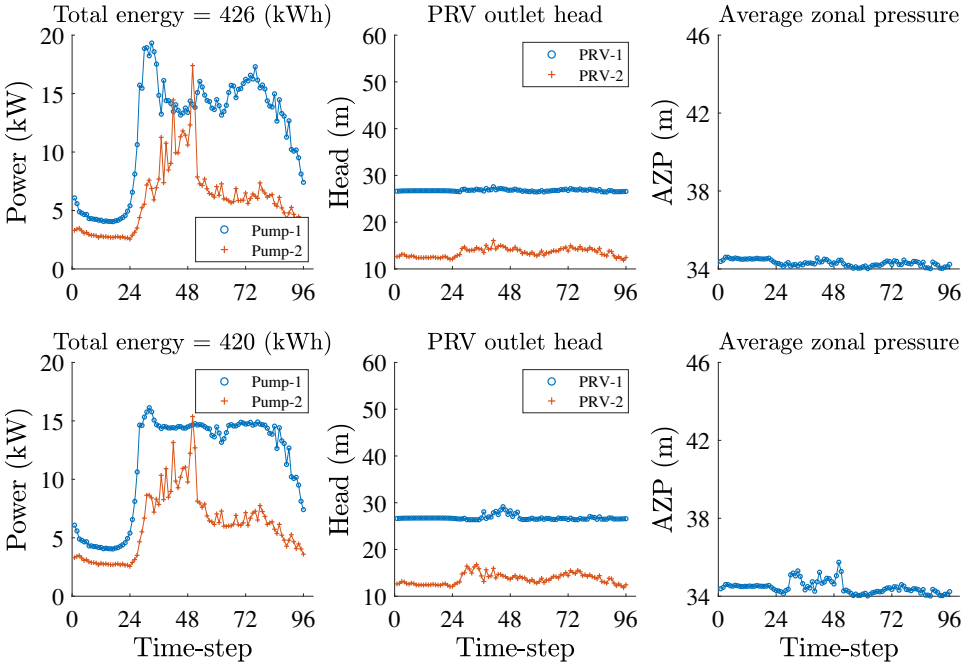

Fig. 5. AZP-optimal operation of the BWFL network. The first row of graphs corresponds to the solution of P1 (no efficiency constraints) and the second row to the solution of P2 (efficiency constraints).

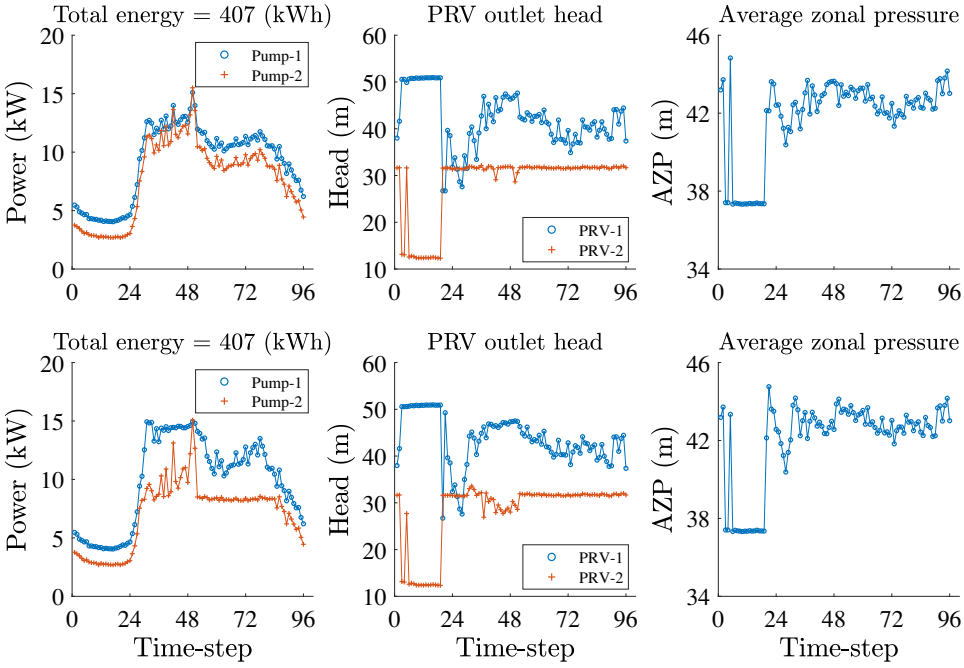

Fig. 6. Energy-optimal operation of the BWFL network. The first row of graphs corresponds to the solution of P1 (no efficiency constraints) and the second row to the solution of P2 (efficiency constraints).

constraints are taken into account, especially for PRV-1 which is practically stable throughout the operations of the WDN when efficiency constraints are not considered.

We next consider the pump energy consumption as our objective function. Given q_j and u_j, using the affinity laws and Eq. (9), of the nominal curve, we can calculate the flow for which, at nominal speed, the pump has the same efficiency as when operating at q_j and u_j and thus, using the efficiency curve (10) calculate $\eta(q_j, u_j)$ and finally the energy consumption at q_j and u_j using formula (12).

However, for our experiments, we have fitted a quadratic polynomial in order to obtain an approximation of the energy consumption surface and use it as our objective function. This, resulted in a convex quadratic polynomial and thus more convenient, with respect to optimization, compared to a more complicated closed formula for the energy consumption. Note however, that this approximation was only used for the optimization. For the results shown in Fig. 4–6 and, the calculation of the energy consumption was performed using formula 12.

In Fig. 6, we show the results from the optimal 24-hour operation of the WDN, acquired by solving problems P1 and P2, with energy consumption (EC) as the objective function. It is evident from the graphs in Fig. 5 that the AZP takes significantly higher

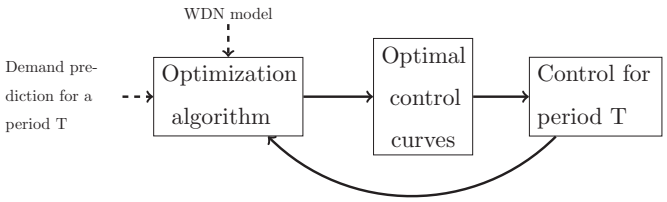

Fig. 7. Automated optimal control scheme.

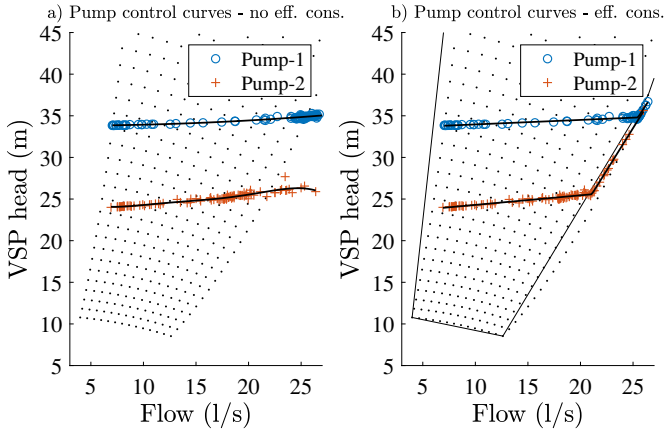

Fig. 8. Inlet flows and outlet heads of the VSPs obtained from solving: (a). P1; and, (b). P2 with AZP as objective. The fitted control curves are shown with solid black lines. The dots indicate the area of efficiency $\geq 55\%$.

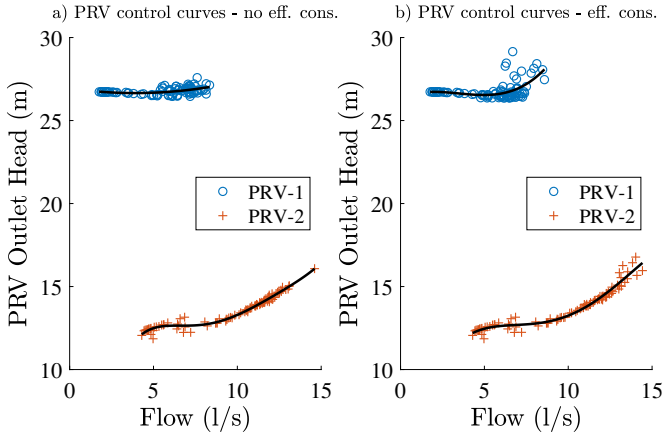

Fig. 9. Inlet flows and outlet heads of the PRVs obtained from solving a) P1 and b) P2 with AZP as objective. The fitted control curves are shown with solid black lines.

values (up to 10m higher) when EC is the objective, while there is little gain in the reduction of total energy use (13kWh or 3%). As as result, for this case study, we do not further consider EC as an objective.

6.2. Automated optimal control of the WDN

In the previous subsection we have presented the results from the solution of problems P1 and P2 with AZP and EC as objectives. However, once the optimization problem is solved, we need to determine how pumps and valves are going to be controlled in practice, during the 24-hour operation of the WDN. In fact, the results have been obtained for a predicted water demand. The uncertainty inherent in water network modelling could cause the computed pump and valve settings to be sub-optimal or even infeasible. We define control curves so that the implemented controls are as close as possible to optimized settings. These curves are fitted to the points (q_t, u_t) obtained from solving the optimization problem (i.e. P1 or P2), where q_t is the inlet flow of a pump or valve and u_t is the corresponding outlet head at time-step t. Sensors placed at the inlet and outlet of pumps and valves measure the inlet flow and outlet pressure. When a measurement of inlet flow is taken, using the control curves, we adjust the operation of the pump or valve until the outlet pressure measurement matches the curve. We refer to this form of feedback control as "flow modulation control" (see Ulanicki, Bounds, Rance, and Reynolds (2000); Wright et al. (2015)).

In order to automatically compute the control curves for VSPs and PRVs, we implement the following strategy: Given the points (q_t, u_t), $t = 1, 2, ..., n_t$ we consider the statistical models,

$$u_t = f_i(q_t) + \varepsilon_t \tag{14}$$

where ε_t are independent random variables with $\varepsilon_t \sim \mathcal{N}(0, \sigma^2)$ and f_i, $i = 1, 2, ..., n_{models}$ are functions, $f_i : \mathcal{A} \subseteq \mathbb{R} \to \mathbb{R}$, of our choice to be fitted to the optimization derived points (q_t, u_t). In our implementation we have considered nth degree polynomials with n=1,...,6, an exponential of the form ae^{bx} and a piece-wise linear function with two segments (the break point of the two segments is also a parameter). In order to consider the trade-off between the SSE (Sum of Squared Errors) of a model and its number of parameters, we make use of the Akaike Information Criterion (AICc) (Akaike, 1998) (see also Burnham and Anderson (1998) pages 63–66). With the assumptions we made for the statistical models in Eq. (14) the AICc value for the statistical model corresponding to f_i is given by

$$AICc_i = n_t ln(SSE_i/n_t) + (2k_i n_t)/(n_t - k_i - 1) \tag{15}$$

where k_i is the number of parameters of f_i plus one for the σ parameter of the residual ε_t. The model with the lowest value of $AICc$ is considered the best and thus the corresponding function, f^*, is the one chosen as our control curve. This procedure is shown in Algorithm 1.

Algorithm 1: Algorithm for automated control-curve fitting.

```
Initialize: minAICc ← ∞;
for i = 1, 2, .., n_models do
    Fit f_i to data (q_t, u_t) by minimizing its SSE_i;
    AICc_i ← n_t ln(SSE_i/n_t) + (2k_i n_t)/(n_t − k_i − 1);
    if AICc_i < minAICc then
        minAICc ← AICc_i;
        f* ← f_i;
    end
end
Return f*;
```

The complete process of optimization, control curve fitting and optimal control of the network can thus be automated. This automated optimal control scheme is illustrated in Fig. 7.

In Fig. 8 and 9, we show the control curves obtained for pumps and PRVs respectively. The plotted data were obtained by solving P1 (no efficiency constraints) and P2 (efficiency constraints) with AZP as the objective function. The control curves are chosen using Algorithm 1.

Note that in Fig. 8(b), the (q_t, u_t) points have shifted in order to follow the efficiency constraints. Furthermore, note that, in this case, Algorithm 1 has chosen the piece-wise linear model for the VSP control-curves. Some of the points in Fig. 8(b) can be seen to be slightly outside of the convex polytope. This is because after the optimization results, we run a hydraulic simulation using the optimal control variable values and the original Hazen-Williams headloss formula for more accurate results.

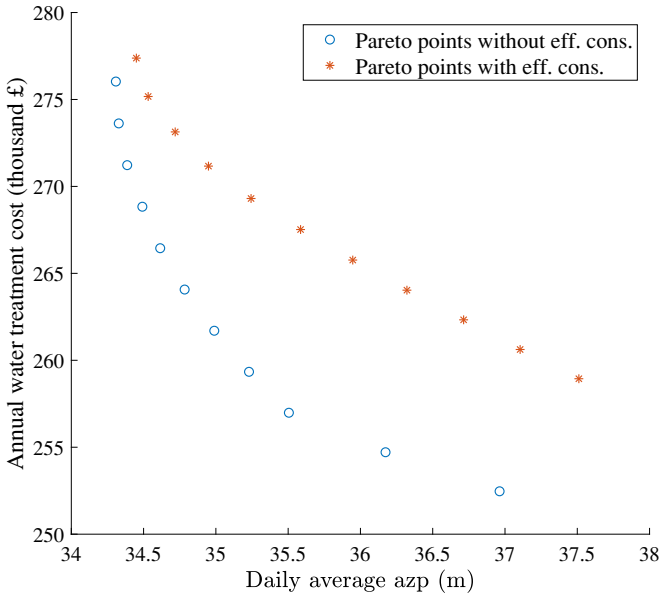

Fig. 10. Pareto-front points obtained from solving Problem P4 with average daily AZP and total WTC as objectives.

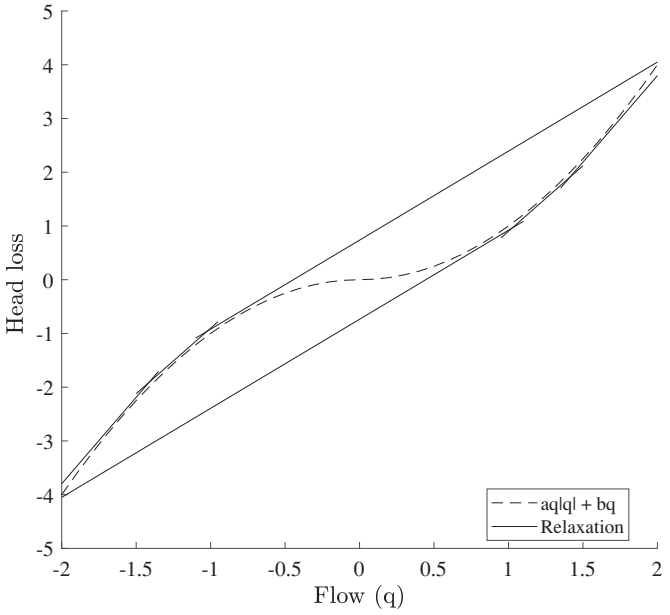

Fig. 11. Example of a polyhedral relaxation for the head loss function $aq|q| + bq$.

6.3. Multi-objective optimal control

By solving P3 for a range of weight vectors $w = [w_1\ w_2]^T$, $w_1 + w_2 = 1$ we obtain the Pareto front points shown in Fig. 10. The fact that the Pareto points without efficiency constraints dominate those obtained when efficiency constraints are included in the formulation is to be expected since, in the latter case, we are solving the same problem but with extra restrictions.

The solutions of the multi-objective problem help us gain useful insights with respect to the optimal operation of the WDN. For example, assuming we are operating the pumps with the efficiency constraints, we see that we can reduce WTC by $\approx$4% (or by $\approx$10, 000 GBP annually) by allowing an increase of one meter pressure head from the minimum AZP value. Moreover, we might decide to install a second pump in each source, in parallel with the existing pump. This will allow us to operate pumps in such a way as to match the results without the efficiency constraints and thus, for the same head increase of 1m, reduce WTC by $\approx$8% (or by $\approx$20, 000 GBP annually).

Finally, note that each Pareto point in Fig. 10 corresponds to a control curve which will allow us to operate the network with the optimized values for AZP and WTC.

6.4. Global optimality bounds

Problems P1 and P2 are non-linear, non-convex problems. However the non-convexities are only due to the terms $a_i q_i |q_i|$ in the energy balance equations. The rest of the terms in the constraints are linear. In addition, all the objective functions considered in this work are convex (AZP and WTC are linear while EC is convex quadratic). Thus, we expect that the solutions provided by IPOPT are global or near-global minima. In this section, we investigate global optimality bounds for the computed solutions. We show that, for the considered problem, the solutions computed by IPOPT are near-globally optimal.

In order to compute global optimality bounds for the solutions of Problem P2, we implement four different global optimization schemes. We evaluate the performance of two state-of-the-art global solvers, BARON v19.3.24 (Tawarmalani & Sahinidis (2005)) and SCIP v5.0.1 (Gleixner et al. (2017)). In addition, we implement a simple branch-and-bound algorithm (with no bound tightening) based on the polyhedral relaxations for the terms $a_i q_i |q_i| + b_i q_i$, presented in Pecci, Abraham, and Stoianov (2018). An example of such a relaxation is shown in Fig. 11.

Furthermore, using the same relaxations, we propose a bound tightening scheme by solving the LP given in Problem 4 (see Puranik and Sahinidis (2017) for a general review of domain reduction techniques).

Problem 4 (P4):

$$
\begin{aligned}
\min\quad & \pm q_i \\
\text{s.t.}\quad & A_{12}^T q - d = 0 \quad \text{(Mass balance)} \\
& g(x) \le 0 \quad \text{(Energy balance linear relaxation)} \\
& Mx \le b \quad \text{(Efficiency constraints)} \\
& q_{min} \le q \le q_{max},\ \ h_{min} \le h \le h_{max} \\
& u \ge 0.
\end{aligned}
$$

where $x = [q\ h\ u]^T \in \mathbb{R}^{n_p+n_n+n_u}$ and $g(x) \le 0$ defines a linear relaxation of the energy balance constraint based on the polyhedral relaxations of the terms $a_i q_i |q_i| + b_i q_i$.

In each round of the bound tightening scheme we solve P4 for all pipes (i.e. flow variables). Note that P4 defines two problems: one with objective $-q_i$ and one with q_i. As soon as one of these problems is solved we update the bounds. At the end of each bound tightening round we use the new bounds to solve a linear relaxation of problem P2 (based on the same relaxations as in P4) and thus obtain a lower bound of the global minimum.

In Fig. 12 we plot the upper and lower bounds calculated, for problem P2 at time-step $t = 45$ with AZP as the objective function. We should mention that SCIP failed to start even after 12 hours (even with the presolving option off) while BARON was unable to calculate an upper bound (this issue with BARON was also reported in Pecci et al. (2018)). Therefore, in Fig. 12 we plot the upper bound calculated by IPOPT and the lower bounds calculated by BARON, our branch-and-bound implementation which we abbreviate as WNBB (Water Network Branch-and-Bound) and the lower bounds obtained by the proposed bound tightening scheme.

As we observe from Fig. 12, both BARON and WNBB fail to provide a conclusive lower bound value. In contrast, after four rounds of the bound tightening scheme we achieve an absolute optimality

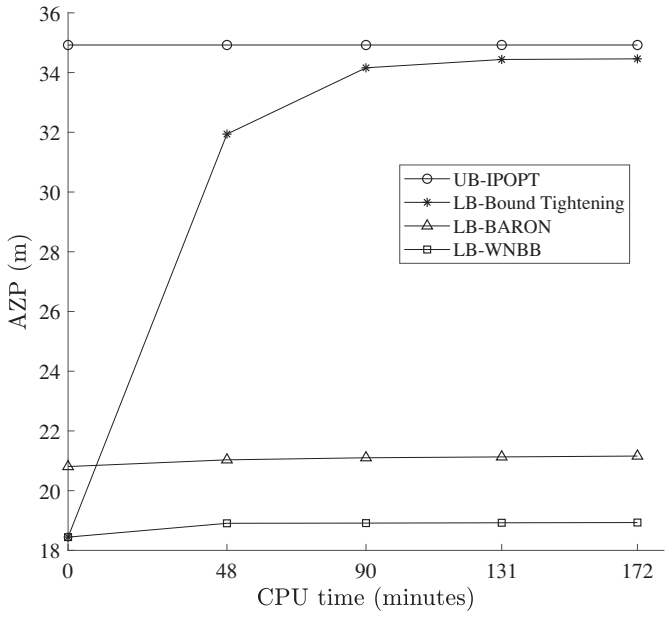

Fig. 12. Bounds (UB = Upper Bound, LB = Lower Bound) for the global minimum of problem P2 with AZP as the objective function at time-step $t = 45$.

Table 1
Comparison (time / GAP%) of the proposed bound tightening scheme and the method presented in Ghaddar et al. (2017).

Network	Valves	Bound Tightening		SDP (Ghaddar et al.)
		Round 1	Round 2	–
Pescara	1	19s / 0.01%	19s / 8e-4%	403s / 3.3e-3%
Pescara	2	19s / 0.02%	19s / 0.01%	384s / 3.8e-3%
Exnet	4	10598s / 51%	11383s / 15%	25529s / 61%

gap of less than 0.5 meters of AZP, which is smaller than the level of uncertainty usually experienced in hydraulic models of water networks. The fact that tailored methods can often outperform general purpose solvers such as BARON and SCIP is also reported in Sahinidis (2019). Moreover, the bound tightening scheme can provide a significant improvement compared to previous work by Ghaddar et al. (2017), where semi-definite programming relaxations for the global solution of valve control in water networks are proposed. A comparison between the two methodologies for the problem of valve control, for the Pescara and Exnet networks from Ghaddar et al. (2017), is shown in Table 1. The placement of the valves in the Pescara network is identical to Ghaddar et al. (2017). For the Exnet network, the placement of the four valves is the same as in Bradley J. Eck (2012). This is because the link id's for the chosen valve locations reported in Ghaddar et al. (2017) do not exist in our version of the Exnet network.

7. Conclusions

The presented optimization problem formulations and solution method are an essential step towards the advanced control of water distribution networks, which dynamically adapt their hydraulic conditions and connectivity in order to achieve multiple operational objectives. This control approach enables water utilities to better respond to the increasing financial, social, environmental and regulatory pressures.

We have presented a methodology for the optimal control of water distribution networks (WDNs) without storage capacity. Using mathematical optimization we formulate and solve the problem of optimal control of variable speed pumps (VSPs) and pressure reducing valves (PRVs). We consider both single and multi-objective formulations.

Using the optimized solutions, we propose a strategy to automatically calculate the control-curves for VSPs and PRVs, which are used to optimally operate the network. We thus propose an optimal control scheme, which provides greater flexibility to manage a wide range of operational conditions and needs.

As a study case, we apply the proposed methodology on a network model based on a real operational network from Bristol, UK, comprised of 2013 nodes and 2369 pipes. As objective functions, we consider the average zonal pressure, the pump energy consumption and the water treatment cost. Both the optimization formulations and the automated control-curve fitting are general and applicable to any network without storage capacity.

The absence of storage elements decouples the problem of optimal control of pumps and valves in time. Thus, it allows us to solve the optimization problem separately and if needed in parallel for each time-step. Although, the problem is non-linear and non-convex, the presented formulation simplifies the modelling of the variable speed pumps without neglecting their physical characteristics. The non-linearities present in the formulation are only due to the head-loss terms. The numerical experiments show that the proposed method can solve (using local solvers) the problem of optimal control of networks without storage in minutes and if needed even in seconds with easily available computational power, when real sized networks are considered. Moreover, we have proposed an optimization based bound tightening scheme to compute global optimality bounds for the considered optimization problems. The results suggest that, for the considered problem, the proposed scheme performs better that previous approaches in the literature as well as state-of-the-art solvers such as BARON and that the solutions computed by the local solver IPOPT are globally or near-globally optimal.

Acknowledgements

This work is fully supported by EPSRC (EP/P004229/1, Dynamically Adaptive and Resilient Water Supply Networks for a Sustainable Future).

Supplementary material

Supplementary material associated with this article can be found, in the online version, at doi:10.1016/j.ejor.2019.12.011.

References

Abraham, E., & Stoianov, I. (2015). Efficient preconditioned iterative methods for hydraulic simulation of large scale water distribution networks. *Procedia Engineering, 119*, 623–632. Computing and Control for the Water Industry (CCWI2015) Sharing the best practice in water management. doi: 10.1016/j.proeng.2015.08.915.

Abraham, E., & Stoianov, I. (2017). Constraint-preconditioned inexact newton method for hydraulic simulation of large-scale water distribution networks. *IEEE Transactions on Control of Network Systems, 4*(3), 610–619. doi:10.1109/TCNS.2016.2548418.

Akaike, H. (1998). Information theory and an extension of the maximum likelihood principle. In *Selected papers of hirotugu akaike* (pp. 199–213). New York: Springer New York. doi:10.1007/978-1-4612-1694-0_15.

Bradley J. Eck, M. M. (2012). Vavle placement in water networks: mixed-integer non-linear optimization with quadratic pipe friction. *Technical Report*. IBM Research.

Bradley J. Eck, M. M. (2015). Quadratic approximations for pipe friction. *Journal of Hydroinformatics, 17*(3), 462–472. doi:10.2166/hydro.2014.170.

Brdys, M., & Ulanicki, B. (1994). *Operational control of water systems: structures, algorithms, and applications*. Prentice Hall.

Burnham, K. P., & Anderson, D. R. (1998). *Model selection and multimodel inference: A practical information-theoretic approach*. New York, NY, USA: Springer New York.

Das, I., & Dennis, J. (1998). Normal-boundary intersection: A new method for generating the pareto surface in nonlinear multicriteria optimization problems. *SIAM Journal on Optimization, 8*(3), 631–657. doi:10.1137/S1052623496307510.

D'Ambrosio, C., Lodi, A., Wiese, S., & Bragalli, C. (2015). Mathematical programming techniques in water network optimization. *European Journal of Operational Research, 243*(3), 774–788. doi:10.1016/j.ejor.2014.12.039.

Fooladivanda, D., & Taylor, J. A. (2018). Energy-optimal pump scheduling and water flow. *IEEE Transactions on Control of Network Systems, 5*(3), 1016–1026. doi:10.1109/TCNS.2017.2670501.

Ghaddar, B., Claeys, M., Mevissen, M., & Eck, B. J. (2017). Polynomial optimization for water networks: Global solutions for the valve setting problem. *European Journal of Operational Research, 261*(2), 450–459. doi:10.1016/j.ejor.2017.03.011.

Ghaddar, B., Naoum-Sawaya, J., Kishimoto, A., Taheri, N., & Eck, B. (2015). A Lagrangian decomposition approach for the pump scheduling problem in water networks. *European Journal of Operational Research, 241*(2), 490–501. doi:10.1016/j.ejor.2014.08.033.

Gleixner, A., Eifler, L., Gally, T., Gamrath, G., Gemander, P., Gottwald, R. L., … Witzig, J. (2017). The SCIP Optimization Suite 5.0. *Technical Report*. Optimization Online.

Lambert, A., & Thornton, J. (2011). The relationships between pressure and bursts - a 'state-of-the-art' update.. *Water 21*, 37–38.

León-Celi, C. F., Iglesias-Rey, P. L., Martínez-Solano, F. J., & Savic, D. (2018). Operation of multiple pumped-water sources with no storage. *Journal of Water Resources Planning and Management, 144*(9), 04018050. doi:10.1061/(ASCE)WR.1943-5452.0000971.

Messac, A., Ismail-Yahaya, A., & Mattson, C. (2003). The normalized normal constraint method for generating the pareto frontier. *Structural and Multidisciplinary Optimization, 25*(2), 86–98. doi:10.1007/s00158-002-0276-1.

Miettinen, K. (1998). *Nonlinear Multiobjective Optimization*. Springer US. doi:10.1007/978-1-4615-5563-6.

Page, P. R., Abu-Mahfouz, A. M., & Mothetha, M. L. (2017). Pressure management of water distribution systems via the remote real-time control of variable speed pumps. *Journal of Water Resources Planning and Management, 143*(8), 04017045. doi:10.1061/(ASCE)WR.1943-5452.0000807.

Pecci, F., Abraham, E., & Stoianov, I. (2017). Quadratic head loss approximations for optimisation problems in water supply networks. *Journal of Hydroinformatics, 19*(4), 493–506.

Pecci, F., Abraham, E., & Stoianov, I. (2018). Global optimality bounds for the placement of control valves in water supply networks. *Optimization and Engineering*. doi:10.1007/s11081-018-9412-7.

Pecci, F., Abraham, E., & Stoianov, I. (2019). Model reduction and outer approximation for optimizing the placement of control valves in complex water networks. *Journal of Water Resources Planning and Management, 145*(5), 04019014. doi:10.1061/(ASCE)WR.1943-5452.0001055.

Puranik, Y., & Sahinidis, N. V. (2017). Domain reduction techniques for global NLP and MINLP optimization. *Constraints, 22*(3), 338–376. doi:10.1007/s10601-016-9267-5.

Sahinidis, N. V. (2019). Mixed-integer nonlinear programming 2018. *Optimization and Engineering, 20*(2), 301–306. doi:10.1007/s11081-019-09438-1.

Skworcow, P., Paluszczyszyn, D., & Ulanicki, B. (2014). Pump schedules optimisation with pressure aspects in complex large-scale water distribution systems. *Drinking Water Engineering and Science, 7*(1), 53–62. doi:10.5194/dwes-7-53-2014.

Tawarmalani, M., & Sahinidis, N. V. (2005). A polyhedral branch-and-cut approach to global optimization. *Mathematical Programming, 103*, 225–249.

Ulanicki, B., Bounds, P., Rance, J., & Reynolds, L. (2000). Open and closed loop pressure control for leakage reduction. *Urban Water, 2*(2), 105–114. doi:10.1016/S1462-0758(00)00048-0. Developments in water distribution systems

Wächter, A., & Biegler, L. T. (2006). On the implementation of an interior-point filter line-search algorithm for large-scale nonlinear programming. *Mathematical Programming, 106*(1), 25–57. doi:10.1007/s10107-004-0559-y.

Walski, T., & Creaco, E. (2016). Selection of pumping configuration for closed water distribution systems. *Journal of Water Resources Planning and Management, 142*(6), 04016009. doi:10.1061/(ASCE)WR.1943-5452.0000635.

Walski, T., Zimmerman, K., Dudinyak, M., & Dileepkumar, P. (2003). Some surprises in estimating the efficiency of variable-speed pumps with the pump affinity laws. In *World water and environmental resources congress* (pp. 1–10). doi:10.1061/40685(2003)137.

Wright, R., Abraham, E., Parpas, P., & Stoianov, I. (2015). Control of water distribution networks with dynamic DMA topology using strictly feasible sequential convex programming. *Water Resources Research, 51*(12), 9925–9941. doi:10.1002/2015WR017466.

Wright, R., Stoianov, I., Parpas, P., Henderson, K., & King, J. (2014). Adaptive water distribution networks with dynamically reconfigurable topology. *Journal of Hydroinformatics, 16*(6), 1280–1301. doi:10.2166/hydro.2014.086.